JOURNAL OF GUIDANCE, CONTROL, AND DYNAMICS
Vol. 18, No. 1, January–February 1995

Engineering Notes

ENGINEERING NOTES are short manuscripts describing new developments or important results of a preliminary nature. These Notes cannot exceed 6 manuscript pages and 3 figures; a page of text may be substituted for a figure and vice versa. After informal review by the editors, they may be published within a few months of the date of receipt. Style requirements are the same as for regular contributions (see inside back cover).

Determination of Piloting Feedback Structures for an Altitude Tracking Task

Norihiro Goto*
Kyushu University, Fukuoka 812, Japan

Introduction

ANALYTICAL assessment of aircraft handling qualities is often based on an assumed feedback structure closed by the pilot. However, there are various situations where the pilot has a choice of feedback structures. For such a situation, it is necessary to determine the structure actually employed by the pilot. An example is the control of the altitude h by the elevator δ_e, which has two possible candidates for the feedback structure shown in Figs. 1a and 1b. Figure 1a is a direct output feedback single-loop system, referred to here as the D model, whereas Fig. 1b is a multiple feedback system with a pitch attitude θ feedback inner loop,[1] referred to as the I model. In Figs. 1a and 1b, Y_p, Y_{p_h}, and $Y_{p\theta}$ are pilot transfer functions, and r_p, r_h, and r_θ are pilot remnants. G is the aircraft dynamics matrix

$$G = \begin{bmatrix} G_{h_{\delta_e}} & G_{\theta_{\delta_e}} \end{bmatrix}^T \tag{1}$$

where $G_{h_{\delta_e}}$ and $G_{\theta_{\delta_e}}$ are the h and θ responses from δ_e. The systems of Figs. 1a and 1b are excited by a vertical gust w_g and a command input h_c. These external signals and pilot remnants are assumed zero-mean, mutually independent random processes. The number of external signals is consistent with the identifiability condition.[2]

Treating this altitude tracking task, this paper is aimed at proposing an identification method capable of determining which is the actual operating feedback structure, the D model or the I model. Reference 3 proposes a method, in which the covariance matrix of the innovations of the autoregressive (AR) model fitted to the data obtained from the feedback system is a key to the judgment on the feedback structure. The application of the method to flight simulation and flight test data, however, does not provide clearcut results. Additional information is needed to make the judgment more definite. This paper proposes a method that utilizes an AR scheme and a singular value analysis of the transfer function matrix from the innovations to the outputs.

Singular Value Analysis

In the AR scheme, the systems of Figs. 1a and 1b are reduced to the feedback structure of Fig. 2. In Fig. 2, the D model has the same structure as the I model does, but the quantities in the blocks are different: for the D model structure, the quantities in the two blocks related to pilot transfer functions and at a summing point are replaced by those in the parentheses. U, V_1, and V_2 are the innovations, which become actual external noises by passing through the shaping filters H_u and H_v. Note that U and $V = [V_1\ V_2]^T$ are mutually uncorrelated.[3]

For the D-model structure, the relationship between the innovations and the outputs $[\delta_e\ h_\varepsilon\ \theta]^T$ reduces to

$$\begin{bmatrix} \delta_e \\ h_\varepsilon \\ \theta \end{bmatrix} = \frac{1}{1 + Y_p G_{h_{\delta_e}}} \begin{bmatrix} * & Y_p H_{v11} & Y_p H_{v12} \\ * & H_{v11} & H_{v12} \\ * & * & * \end{bmatrix} \begin{bmatrix} U \\ V_1 \\ V_2 \end{bmatrix} \tag{2}$$

where

$$H_v = \begin{bmatrix} H_{v_{ij}} \end{bmatrix}, \qquad i = 1, 2 \qquad \text{and} \quad j = 1, 2 \tag{3}$$

The salient feature of Eq. (2) associated with the nonexistence of the inner-loop transfer function $Y_{p\theta}$ in the D model is that the matrix enclosed by a broken line is singular. It can be easily shown that the I model does not make this singularity. Since in actuality the numerical procedure of the identification may bring about a nonzero value of the determinant of the matrix, it is common practice to test the singularity by using the singular values of the matrix.[4] Assume that an AR model of the form of Eq. (2) is fitted to the observed data $X(n) = [\delta_e(n)\, h_\varepsilon(n)\, \theta(n)]^T$ as[3]

$$X(n) = L(B)\mathrm{W}(n) \tag{4}$$

where W(n) is the innovation vector, n is the sampling instant, $n = 1, 2, \ldots$, and $L(B)$ is the transfer function matrix described in terms of the backward shift operator B. Then, two singular values can be obtained from the matrix in $L(B)$ corresponding to that enclosed by the broken line in Eq. (2). To compute the singular values, B is replaced by $\exp(-j\omega T_s)$, where ω is the frequency in rad per second, T_s is the sampling interval in seconds, and $j = \sqrt{-1}$. Let the larger and smaller singular values of the matrix be σ_L and σ_S. The ratio σ_S/σ_L should be very small if the system has a D-model structure, whereas it should take a significant value if the system has an I-model structure. Note that the

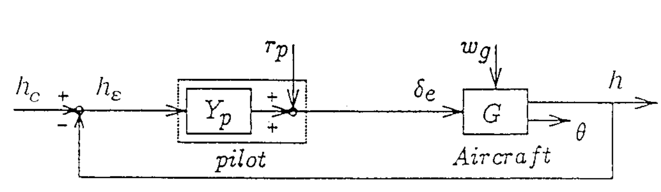

a)

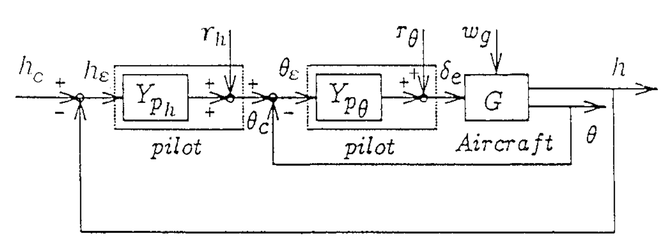

b)

Fig. 1 Feedback structures for an altitude tracking task: a) direct altitude feedback single loop, D model and b) multiple loop with a pitch attitude control inner loop, I model.

Presented as Paper 93-3669 at the AIAA Atmospheric Flight Mechanics Conference, Monterey, CA, Aug. 9–11, 1993; received Nov. 1, 1993; revision received June 4, 1994; accepted for publication June 28, 1994.

*Professor, Department of Aeronautics and Astronautics. Associate Fellow AIAA.

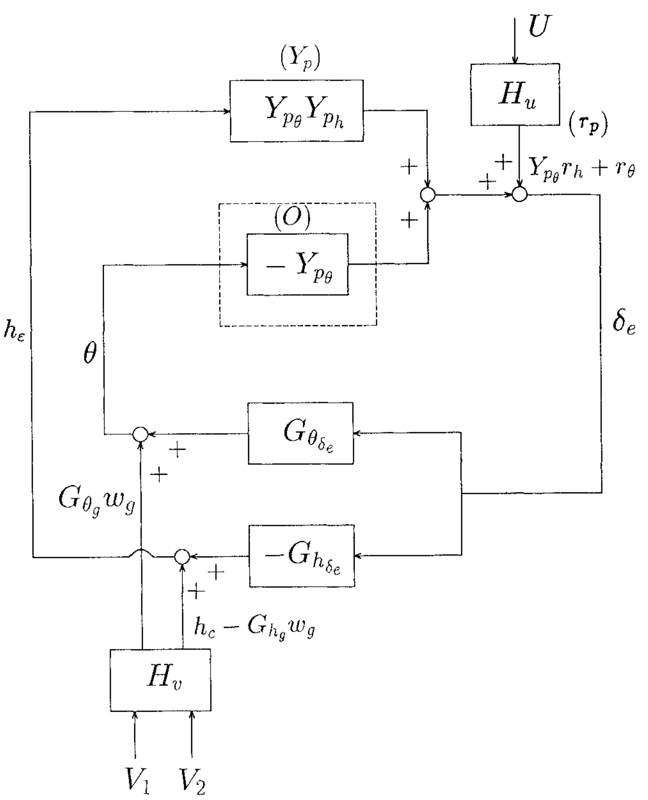

Fig. 2 D and I models fitted to the AR structure.

ratio is nondimensional and a function of the frequency. Based on the consideration made thus far, the singularity test is proposed here as a method to judge the system structure. To summarize, if the singular value ratio is very small, the D model is the correct structure.

Computer Analysis

To validate the proposed method, a computer analysis was conducted. In the work, D and I models of an altitude tracking task were realized on a digital computer to acquire the data (δ_e, h_ε, θ). The simulated aircraft was the Navion[5] with the same flight configuration and aircraft transfer functions as listed in Ref. 3. A vertical gust having the one-dimensional Dryden spectral form of the intensity $\sigma_w = 1.0$ ft/s (0.3 m/s) and the scale length $L_w = 460$ ft (140 m) was applied to the aircraft. The gust generation process is illustrated in Fig. 3 together with those of pilot remnants and a command input. $Z_1 \sim Z_4$ in Fig. 3 are mutually independent Gaussian white noises with unit rms. Referring to Figs. 1a and 1b, the simulated pilot transfer functions are

$$Y_p = K_p e^{-\tau s}(1 + T_L s)/(1 + T_I s) \tag{5}$$

$$Y_{p_h} = K_{p_h} \tag{6}$$

$$Y_{p_\theta} = K_{p_\theta} e^{-\tau s}(1 + 0.2s)/(1 + 0.1s) \tag{7}$$

$$\tau = 0.06s \tag{8}$$

Parameters (K_p, T_L, T_I) of Eq. (5) and (K_{p_h}, K_{p_θ}) of Eqs. (6) and (7) were the experimental variables. Numerical values of these parameters are given in Table 1 for the D model and in Table 2 for the I model with a simulation number assigned to each combination of the parameters. These parameter values were selected so that the stability of the system exceeded a certain level. The intensity of the pilot remnant injected in generating δ_e was also changed through C_θ in Fig. 3. Other parameters were fixed: $C_h = 0.001$, $C_{h_c} = 0.1$, and $\omega_1 = 3.14$ rad/s. These parameter values of the noises were based on an analysis of the signal to noise ratio. The transfer functions in continuous form were reduced to the zero-order hold

Table 1 Parameter values and simulation numbers for D-model simulation

T_I	T_L / K_P	6.0	8.0	10.0	12.0	14.0
0.0015	K_P	−0.000012	−0.00001	−0.000008	−0.000006	−0.000006
	No.	1	6	11	16	21
0.0012	K_P	−0.000012	−0.00001	−0.000008	−0.000006	−0.000006
	No.	2	7	12	17	22
0.0010	K_P	−0.000012	−0.00001	−0.000008	−0.000006	−0.000006
	No.	3	8	13	18	23
0.0008	K_P	−0.000012	−0.00001	−0.000008	−0.000006	−0.000006
	No.	4	9	14	19	24
0.0005	K_P	−0.000012	−0.00001	−0.000008	−0.000006	−0.000006
	No.	5	10	15	20	25

Table 2 Parameter values and simulation numbers for I-model simulation

K_{p_h} \ K_{p_θ}	−0.5	−1.0	−2.0	−4.0
0.008	1	2	4	7
0.009	—	3	5	8
0.012	—	—	6	9
0.015	—	—	—	10

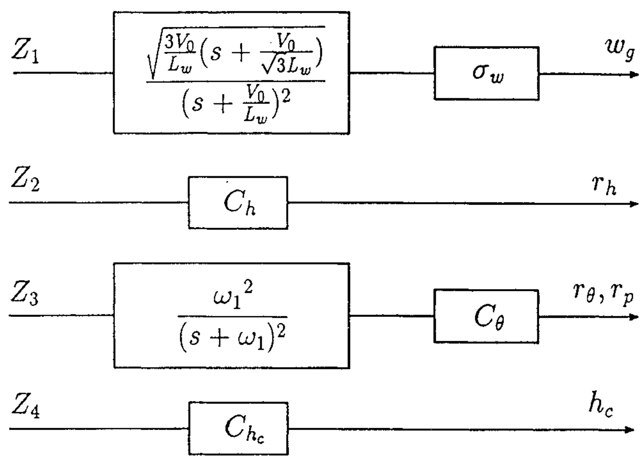

Fig. 3 Generation of external noises.

pulse transfer functions. Each of the data contained 1600 computed points, but 1400 points were subjected to the analysis, excluding the initial 200 points. The sampling time T_s was set equal to 0.06 s.

Figures 4a and 4b show examples of the results of the singular value analysis. The singular value ratio σ_S/σ_L is plotted in the frequency range $\omega_0 \le \omega \le 40\ \omega_0$, where $\omega_0 = \omega_N/200$, and ω_N is the Nyquist frequency. The slanted axes indicate the simulation numbers of Tables 1 and 2. Figure 4a exhibits clearly

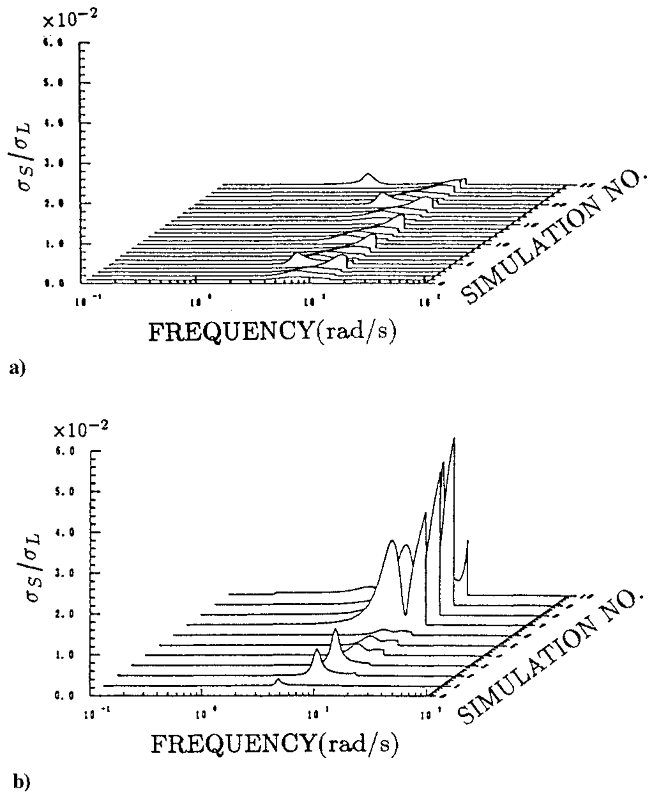

Fig. 4 Results of the singular value analysis: a) D-model simulation, $C_\theta = 0.02$, and b) I-model simulation, $C_\theta = 0.02$.

that for all cases of the D-model simulation the matrix enclosed by a broken line in Eq. (2) is almost singular, suggesting that the D model is the correct structure. On the other hand, Fig. 4b shows that the singular value ratio takes significant values in the frequency range of interest if the inner-loop gain K_{p_θ} is large enough. A close look at Fig. 4b and an analysis can point out the following: a peak exists around the short period mode natural frequency, the peak magnitude increases as the magnitude of Y_{p_h} increases, and the frequency band where the singular value ratio takes significant values shrinks as the pilot remnant intensity increases.

Conclusions

An identification method is proposed to determine the feedback structure employed by the pilot in a system with a choice of feedback structures. The method utilizes an autoregressive scheme and a singular value analysis. The method is applied to an analysis of the computer simulation data of an altitude tracking task. It is shown that the method can make clear judgment on the feedback structure. Application to the data from the real world is to be made in the future.

References

[1]Chalk, C. R., "Flying Qualities of Pitch Rate Command/Attitude Hold Control System for Landing," *Journal of Guidance, Control, and Dynamics*, Vol. 9, No. 5, 1986, pp. 541–545.

[2]Ng, T. S., Goodwin, G. C., and Anderson, B. D. O., "Identifiability of MIMO Linear Dynamic Systems Operating in Closed Loop," *Automatica*, Vol. 13, 1977, pp. 477–485.

[3]Goto, N., and Matsuo, T., "Identification of Pilot Dynamics in a System with a Choice of Feedback Structures," *Journal of Guidance, Control, and Dynamics*, Vol. 11, No. 2, 1988, pp. 159–166.

[4]Stengel, R. F., *Stochastic Optimal Control—Theory and Application*, Wiley, New York, 1986, pp. 591–595

[5]Teper, G. L., "Aircraft Stability and Control Data," STI Tech. Rept. 176-1, Systems Technology, Hawthorne, CA, 1969, pp. 93–103.

Dynamics and Control of Slewing Active Beam

Moon K. Kwak,* Keith K. Denoyer,† and Dino Sciulli‡
Phillips Laboratory,
Kirtland Air Force Base, New Mexico 87117

I. Introduction

THE performance requirements of future space systems have brought much attention to the study of the simultaneous slewing and vibration suppression of space structures. To fulfill the requirements of precision spacecraft, the aerospace community has been looking for active structures, i.e., structures with highly integrated sensors and actuators, which can be used to change the mechanical properties of the structure.[1–5]

In this Note, a slewing flexible beam equipped with a multitude of piezoelectric sensox xxrs and actuators is modeled by use of the extended Hamilton principle, resulting in the equations of motion as well as the measurement equations. Nonlinearity enters into the equations of motion through the rigid-body rotational motion, whereas the elastic vibration is assumed to be small compared to the rigid-body rotation. Based on these equations, the decentralized control concept is proposed, which divides controls into the slewing and vibration suppression control. Slewing is achieved by utilizing sliding-mode control[6] as if the system were rigid and the vibration suppression is carried out independently by means of modal-space positive-position-feedback control[7] plus disturbance counteracting control.

All the developments in this paper are verified by the experiment.

II. Modeling of Slewing Active Beam

The motion of the beam is constrained to a horizontal plane and the beam is thin compared to its length so that we can regard it as an Euler-Bernoulli beam. Placed on the beam are piezoceramic plates that can be used as sensors or actuators. To model such a beam, we need to combine the stress-strain relationship of the Euler-Bernoulli beam theory with the piezoelectric constitutive equation. The control design for the hybrid equation is not feasible, so that the elastic displacement is discretized by introducing the admissible functions

$$v = v(x, t) = \sum_{j=1}^{n} \phi_j(x) q_j(t) = \Phi \boldsymbol{q} \tag{1}$$

where $v(x, t)$ is the elastic displacement of the beam, $\Phi = [\phi_1 \quad \phi_2 \ldots \phi_n]$ is a vector of assumed mode shape, $\boldsymbol{q} = [q_1 \; q_2 \ldots q_n\;]^T$ are generalized coordinates, and n is the number of assumed modes, respectively. We assume that the admissible function introduced in Eq. (1) automatically satisfies the boundary conditions. Thus, the total kinetic energy can then be written as

$$T = \tfrac{1}{2} J \dot{\theta}^2 + \tfrac{1}{2} \dot{\theta}^2 \boldsymbol{q}^T M \boldsymbol{q} + \dot{\theta} \tilde{\Phi} \dot{\boldsymbol{q}} + \tfrac{1}{2} \dot{\boldsymbol{q}}^T M \dot{\boldsymbol{q}} \tag{2}$$

where θ is the slewing angle, J is the total mass moment of inertia, M is the total mass matrix, $\tilde{\Phi} = \int \bar{m} x \Phi \, dx$ in which $\bar{m}$ is the mass density, respectively. In addition, the total virtual work has the form

$$\delta W = \delta \boldsymbol{v}^T C \boldsymbol{v} - \delta \boldsymbol{v}^T B^T \boldsymbol{q} - \delta \boldsymbol{q}^T B \boldsymbol{v} - \delta \boldsymbol{q}^T K \boldsymbol{q} + T_h \delta\theta \tag{3}$$

where $\boldsymbol{v}$ is the voltage applied or generated in the piezoceramic plate, B and C are coefficient matrices resulting from the piezoelectric property of the piezoceramic plates, K is the total stiffness

Received June 3, 1993; revision received April 19, 1994; accepted for publication April 20, 1994.

*Research Assistant Professor, Department of Mechanical Engineering, University of New Mexico. Member AIAA.

†Mechanical Engineer, Structures and Control Division.

‡Aerospace Engineer, Structures and Control Division. Member AIAA.